
EFFECT OF COPPER ON THE INITIAL STAGE SINTERING OF ALUMINA

A thesis submitted in the partial fulfilment of the requirements
for the degree of Bachelor of Technology

By

PRAVASISH NAYAK

109CR0540



EFFECT OF COPPER ON THE INITIAL STAGE SINTERING OF ALUMINA

A thesis submitted in the partial fulfilment of the requirements

for the degree of Bachelor of Technology

By

PRAVASISH NAYAK

109CR0540

Supervisor:

Dr. Shantanu Behera





NATIONAL INSTITUTE OF TECHNOLOGY, ROURKELA

CERTIFICATE

This is to certify that the thesis entitled, “**EFFECT OF COPPER ON THE INITIAL STAGE SINTERING OF ALUMINA**” submitted by **Mr. PRAVASISH NAYAK (109CR0540)** in partial fulfilment for the requirements for the award of Bachelor of Technology degree in Ceramic Engineering at National Institute of Technology, Rourkela is an authentic work carried out by him under my supervision and guidance.

To the best of my knowledge, the matter embodied in this thesis has not been submitted to any other University/Institute for the award of any Degree or Diploma.

Date:

Dr. Shantanu Behera

Assistant Professor

Department of Ceramic Engineering

National Institute of Technology

Rourkela – 769008.

ACKNOWLEDGEMENT

I acknowledge and I am thoroughly indebted to all those who have been instrumental in helping me out with the various facets of my project.

I sincerely thank my guide **Dr Shantanu K. Behera** for his guidance without whom this project wouldn't have been possible. I would also like to thank our HOD **Dr Swadesh K. Pratihara** who has helped me overcome many difficulties that I faced with the project.

I express my heartfelt thanks to **Dr. S. Bhattacharyya, Dr. B.B Nayak, Dr. D. Sarkar, Dr R. Sarkar, Dr. S. Pal, Dr S. Dasgupta, Dr R. Mazumdar, Dr S. Bhattacharya and Mr Arun Chowdhary** for all their help.

I thank all the laboratory in charges **Mr. Gopinath Behera , Mr.P.K.Mohanty, Mr Susil Sahoo and Mr N Barik** for their support and help in the laboratory jobs that were an integral part of this project.

I would also like to express my gratitude for all the research and PhD scholars especially **Mr. Ganesh Sahoo, Mr. Sanjay Swain, Miss Gitanjali Parida, Mr. Subrat Kumar, Mr. Nadiya Bihari Nayak, Mr. Sarat Kumar Sahoo and Miss Prativa Adhikary** for extending the much needed hand of support and technical help throughout the entire duration of this project.

Last but not the least I thank almighty, my parents and near and dear ones for being a strong pillar of emotional and financial support during this endeavour of mine.

PRAVASISH NAYAK

ROLL NO:- 109CR0540

DEPARTMENT OF CERAMIC ENGINEERING

NIT ROURKELA

CONTENTS

Chapter 1: INTRODUCTION	1
Chapter 2: LITERATURE REVIEW	4
Chapter 3: EXPERIMENTAL	10
3.1 Fabrication Of Powders	11
3.2 Characterization	13
Chapter 4: RESULTS AND DISCUSSION.....	15
4.1 Densification analysis	16
4.2 Dilatometric Study.....	19
4.3 Calculation Of Activation Energy.....	23
4.4 SEM Analysis	29
Chapter 5: SUMMARY.....	32
REFERENCES.....	34

LIST OF TABLES

Table 1: Dependence of frequency factor with temperature corresponding to the kinetics models used in literature	24
Table-2: Values of X And Y Axes for Activation Energy Plot.....	27

LIST OF FIGURES

Fig-1: Fabrication of powders	13
Fig-2: Plot of Bulk Density vs Firing Temperature (soaking time: 4 hrs)-----	16
Fig-3: Plot of Bulk Density with soaking time (temperature : 1650 °C)-----	16
Fig-4: Plot of Apparent Porosity with Firing temperature (soaking time : 4 hrs)-----	17
Fig-5: Plot of Apparent Porosity with soaking time (firing temperature = 1650 °C)-----	18
Fig-6(a): Plot of dL/Lo (shrinkage) with temperature (at 5 °C/min)-----	19
Fig-6(b): Plot of dL/Lo (shrinkage) with time (at 5 °C/min)-----	19
Fig-7(a) : Plot of dL/Lo (shrinkage) with temperature (at 10 °C/min)-----	20
Fig-7(b): Plot of dL/Lo (shrinkage) with time (at 10 °C/min)-----	20
Fig -8(a): Plot of dL/Lo (shrinkage) with temperature (at 15 °C/min)-----	21
Fig- 8(b): Plot of dL/Lo (shrinkage) with time (at 15 °C/min)-----	21
Fig- 9(a) : Plot of dL/Lo (shrinkage) with temperature (stack)-----	22
Fig- 9(b): Plot of dL/Lo (shrinkage) with time (stack)-----	22
Fig-10: Plot of a dilatometric curve for constant heating rate-----	23
Fig-11: Plot of scatter points for activation energy calculation	26
Fig-12: Plot of activation energy graph	27

Fig-13 : Image Of Cu-doped Alumina Fired At 1650 °C With 8 Hrs Soaking Time-----28

Fig-14 : Image Of Cu-doped Alumina Fired At 1650 °C With 10 Hrs Soaking Time-----29

Fig-15: Image Of Alumina Fired At 1650 °C With 10 Hrs Soaking Time -----30

Fig-16: Image Of Cu-doped Alumina Fired At 1650 °C with 12 Hrs Soaking Time-----30

Fig-17: Image of Alumina Fired At 1650 °C with 12 Hrs Soaking Time -----31

ABSTRACT

Study of densification of alumina in the presence of CuO has been studied. CuO as dopant is added to the extent of 0.5 mole % (1 wt%) to pure alumina (A17NE) and studies were done for pressure less sintering. Cold pressed pellets of alumina with or without copper oxide were sintered at 1100 °C, 1200 °C, 1400 °C, 1550 °C and for 1650 °C and were also kept for different soaking time at 1650 °C. The pellets were then characterized for densification and microstructure analysis using SEM. Dilatometric studies were also done on the doped samples. Results showed that doped samples acquire better density (~95% of theoretical density) than undoped samples (~93% of theoretical density). Activation energy calculated for the initial stage of sintering for Cu doped alumina was found to be 329.45kJ/mol. The same for undoped alumina could not be possible due to time constraints.

CHAPTER 1

INTRODUCTION

Aluminium Oxide (Al_2O_3) or alumina is one of the most important ceramic oxides with a variety of applications. It has several crystalline phases, all of which ultimately form the most stable phase rhombohedral alpha alumina at elevated temperatures. This phase is considered best for structural applications. Alpha alumina is one of the stiffest among the oxide ceramics. Its wide range of properties like refractoriness, high hardness, good thermal properties and excellent dielectric properties, allow it to be used in variety of applications. Corundum has rhombohedral crystals with hexagonal structure. The close packing of the aluminium and oxygen atoms within its structure is responsible for its good mechanical and thermal properties. The unit cell is an acute rhombohedron of side length 5.2\AA and plane angle $\sim 55^\circ$.

Since most of the application of alpha alumina is in the structural ceramic components, fabrication of a dense body is highly essential. Many studies have been done on the sintering of alumina, so as to develop a highly dense body with high strength and fracture toughness. This can be done by two ways. The first approach is to optimize fabrication parameters, such as, sintering time, temperature, particle morphology and granulometry. The other approach is the design of microstructure with the use of dopants in the sintering of alumina.

Today the most beneficial sintering aid for alumina is said to be MgO as it helps in inhibiting grain growth, maintains an equiaxed microstructure, and leads to high densification. MgO is believed to decrease the boundary mobility of alumina thus preventing pore boundary separation that effectively eliminates porosity.

Apart from MgO a lot of other additives have also been studied like CaO and SiO_2 . But unlike magnesia they have not been proved to be of much use as they produce abnormal grains, thus deteriorating mechanical properties.

Doping is not only used for densification but also for manipulating the microstructure of alumina that affects not only mechanical properties but also dielectric and optical properties.

For some time now it has been noticed that some rare earth metals and transition metals have shown excellent promise in microstructure development in alumina.

Here in this thesis, we've have worked with Copper (II) oxide which has a melting temperature around 1326 °C. Thus we expect, that at higher temperatures, CuO melts to form a liquid phase. However, the amount of CuO we have added doesn't qualify the system to be called as classical liquid phase sintering. Recent results have shown that formation of intergranular liquid like layers can dramatically influence diffusion processes and microstructure development. Based on these recent works we hope to be able to see a considerable change in densification behaviour in copper doped alumina system.

CHAPTER 2

LITERATURE SURVEY

Various studies [1-4] have been done on the sintering of alumina or alumina based ceramics. It has been observed that a firing temperature above 1600 °C is required for high densification. It has been shown that certain additives when added in requisite amount can lead to enhanced densification at considerably lower temperatures.

A Bettinelli et al[5] investigated the effect of silicate (CaSiO_3) addition on the densification of undoped α alumina. They observed a maximum of 95% theoretical density at a firing temperature of 1400 °C/ 4 hours by liquid phase sintering route. An optimum amount of 2.25 wt% of CaSiO_3 was used. Densification kinetics were also studied for the addition of transitional metal oxides (TiO_2 , Nb_2O_5 , MoO_3) to alumina containing a low melting flux in presence of a reducing atmosphere but it was found it had more or less no effect on the density of the samples.

Hilkat Erkalfa et al [6], investigated the effects of MnO_2 and TiO_2 additions on the sintering of $\alpha\text{-Al}_2\text{O}_3$. Additive combinations in the ratio of 3 wt% MnO_2 + (0.5, 1.5, 3.0) wt% TiO_2 were added and microstructural development as well as microhardness were characterized. The best densification results were reported for the composition Al_2O_3 + 3 wt% MnO_2 + 0.5 wt% TiO_2 (98% of the theoretical density) with a uniform grained microstructure at a temperature of 1250°C. The hardness value obtained was 23.14 GPa at the same temperature conditions.

H. Erkalfa et al [7], studied the effect of additives on the densification and microstructural development of low-grade alumina powders. These alumina powders were produced as an electro filter residue during the Bayer process. Their densification and microstructural evolution were studied using a variety of sintering additives like MnO_2 , SiO_2 , TiO_2 and MgO . The homogeneous mixing of alumina powders and additives was ensured by a colloidal technique and the powders were calcined, hot washed and recalcined to improve the powder quality. Due to

the above processes microstructures with densities between 90-96.7% of the theoretical density were obtained. It was reported that with the addition of the composition 1.5%MnO₂- 0.1%TiO₂- 0.5%MgO - 2%SiO₂ a homogeneously-distributed finer grain size was obtained. Strength values as high as 180- 380 Mpa were obtained in the said specimens.

Coble [8], was the first to report that the addition of magnesia (0.25 wt%) to alumina enabled it to reach near theoretical density. Various literatures have suggested various mechanisms by which MgO helps in inhibiting grain growth. Some literatures reported that MgO increases the rate of densification by increasing the value of grain boundary diffusion coefficient [8,9]. In addition to that , it has also been reported that MgO enhances densification by lowering of the surface diffusion[10].

There have been also various studies that reported that suggest MgO lowers the grain boundary mobility thus inhibiting pore boundary separation, thus decreasing grain growth rate [12-15]. This particular mechanism has now been widely accepted. Although the exact mechanisms to how magnesia addition enhances densification is still contentious.

Radonjić et al [16], studied the effect of MgO doping on the densification of alumina. Its effect on the grain growth of alumina were also studied. It was observed that magnesia addition increased the densification kinetics of alumina but decreased the grain growth rate. It was observed that the main function of magnesia addition was to decrease the particle size during phase transformation and grain growth during sintering.

Yung fu Su et al [17], have studied the effect of niobium doping on the densification and grain growth of nano-sized α -Al₂O₃ powders during sintering. The concentration of the dopant added was in the range 0.1 to 0.5 mol%. It was observed that addition of Nb₂O₅ could improve the densification of the pure alumina with a lower sintering temperature and with less soaking time.

The effect is strengthened by the increase in the amount of dopant. It is also observed that niobium doping significantly enhances the grain growth of alumina during sintering and with increase in the amount of dopant in the given range the grain size of alumina is said to have increased.

Atsushi Odaka et al [18], studied the effect of rare earth (Lu, Gd, Nd) metal doping on the densification of alumina nanopowders obtained by a sol-gel route by seeding. The densification results were best obtained for Lu doped nanopowders with full densification being obtained at 1400 °C by pressureless sintering. The microstructure obtained was observed to be fine grained.

Atsushi Odaka et al [19], demonstrated the effect on the densification of alumina nanopowders due to calcium doping. It has been demonstrated that Ca doped alumina nanopowders which were obtained through a sol-gel route using polyhydroxoaluminum (PHA) and CaCl_2 solutions under α -alumina seeding were able to produce fine-grained ceramics. Appropriate composition for producing the above for low-temperature finer grained densification were 0.10 mol% Ca-doping, 5 mass% α -alumina seeding. Then calcination was done at a temperature of 900 °C. New nano-sized alumina powders were produced, which consisted of α -alumina particles and α -alumina nanoparticles with an average grain size of 80 nm. By use of these Ca-doped nanopowders, fully densified alumina ceramics with a uniform microstructure were produced with an average grain size of 0.66 μm obtained at 1375 °C. Thus it was clearly demonstrated that the proposed sol- gel route for preparing Ca-doped nanopowders was very suitable for fabricating dense, fine-grained alumina ceramics. Undoped samples with 5 mass% seeds had a microstructure with an average grain size of 1.39 μm at 1375 °C.

R. Voytovych et al [20], studied the grain growth and densification in very high-purity α -alumina which were doped with varying amounts of yttrium (0 to 3000 wt% ppm of yttria) and were sintered in air at 1450, 1550 and 1650 °C. It was reported that yttrium doping inhibited densification and coarsening at 1450 °C, but had very little effect at 1550 °C and no effect at 1650 °C. This change in densification behaviour is suggested to be related to the transition with increasing temperature from grain boundary diffusion to lattice diffusion controlled densification. It was also observed that the coarsening rate increases faster with temperature than the densification rate. This was said to be correlated with the higher measured activation energy for grain growth than for the diffusion processes, which control the densification.

Ivan b. Cutler et al [21], studied the bend strength of pure and doped MgO and Al₂O₃. MgO was doped with NiO and cobalt oxide, both forming a complete series of solid solutions with magnesia. The Al₂O₃ was doped with Fe₂O₃ and TiO₂ which has limited solid solubility in Al₂O₃ and with Cr₂O₃ which forms a complete series of solid solutions with alumina. The modulus of rupture (MOR) was correlated to a standard grain size and porosity so as to determine effect of the intrinsic effects of the impurities on it. The results reported that due to the formation of NiO-MgO and CoO-MgO solid solutions, strength of MgO has increased. However, the formation of Cr₂O₃-Al₂O₃, Fe₂O₃-Al₂O₃, and TiO₂-Al₂O₃ solid solutions, had no intrinsic effect on the strength of sintered alumina.

Ivan B. Cutler et al [22], reported that both small particles and the addition of certain oxides enhance the sintering of alumina at temperatures below 1700 °C. By varying combinations of oxides and small particle size, the temperature for sintering of 96% dense alumina bodies was reduced in this investigation to the 1300° to 1400°C range. It is proposed that due to the

formation of a liquid phase the temperature of sintering is reduced. Thin sections of the alumina sintered at low temperatures when observed revealed bodies with small grain size with bulk densities above 3.80 g/cc.

The objectives of the work can be itemized as below:

- To study the densification behaviour of Cu doped alumina samples at different temperatures
- To study the microstructure of Cu doped alumina samples at different temperatures
- To calculate the activation energy of the initial stage of sintering of Cu doped alumina samples.

CHAPTER 3

EXPERIMENTS

3.1 Fabrication of samples:

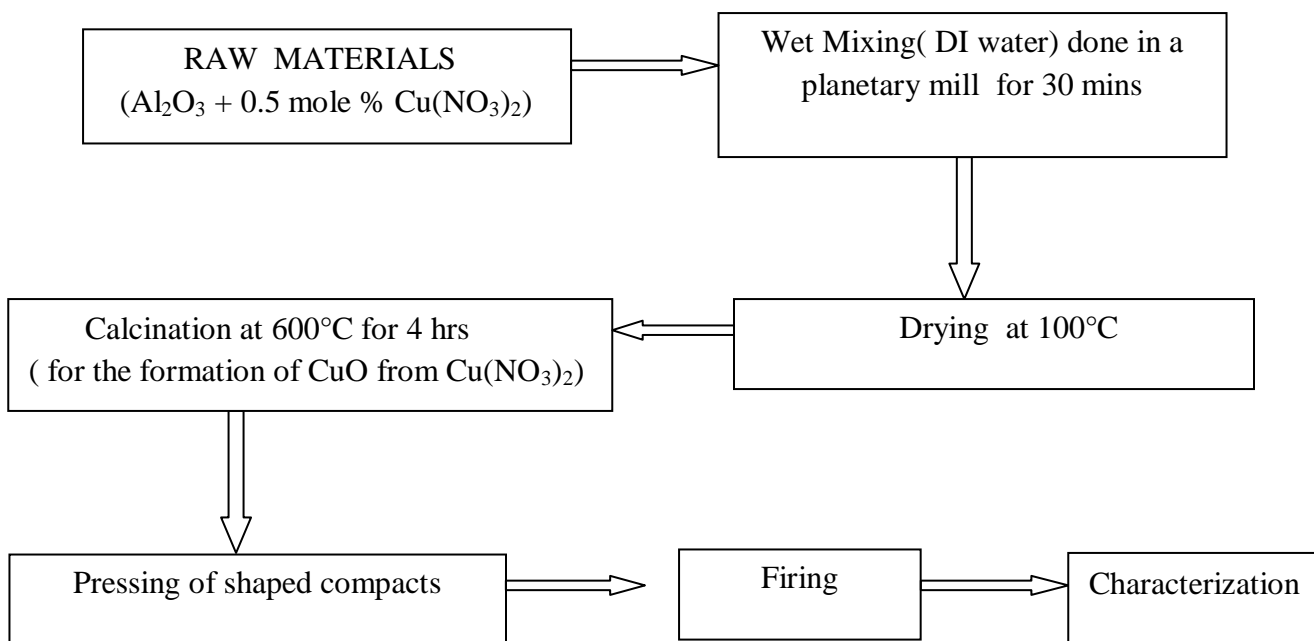


Fig 1. Fabrication of samples

A17NE grade refractory alumina was obtained from Almatiss. It has a 99.8 % purity. It has a bimodal grain size distribution. It has a surface area of 2.9 m²/g and a D50 of 2.6 μm.

Copper (II) nitrate was obtained from Loba chemicals. Copper (II) nitrate is highly hygroscopic in nature, thus it should be kept in an air tight container to prevent its hydration.

We have doped alumina and copper (II) nitrate in a molar ratio 0.5%.

As $\frac{Al}{Cu} = 0.5\%$ (i.e. we have doped according to metal1: metal2 ratio)

As 1 mole of aluminium is obtained from 1 mole of alumina and 1 mole of copper is obtained from 1 mole of Cu(NO₃)₂.

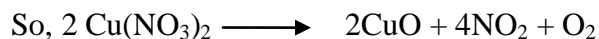
Therefore (Alumina) / (copper (II) nitrate) = 0.5 mole % = 0.005 moles.

So , 50 g of alumina = 0.005 moles of copper nitrate = 0.005 * 241.60 = 1.208 g

Therefore $\frac{\text{copper (II)nitrate}}{\text{alumina}} = 2.4 \text{ wt\%}$

Now after calcination :

Copper (II) nitrate changes into copper (II) oxide,



Here 1 mole of copper (II) nitrate gives 1 mole of copper (II) oxide.

187.56 g/mol of copper (II) nitrate gives 79.54 g/ mol of copper (II) oxide.

Therefore 1.208 g of copper (II) nitrate gives 0.512 g of copper (II) oxide.

Therefore actual dopant percentage :

$$\frac{\text{copper (II) oxide}}{\text{alumina}} = 0.512/50 = 1.02 \text{ wt \%}$$

Mixing was done in a planetary mill in which stainless steel bowls were used with stainless steel balls for mixing (10 large balls and 15 small balls each for each bowl). 2 batches of 35 g of Al_2O_3 each were added to both the bowls. 0.829 gm of $\text{Cu(NO}_3)_2$ (0.5 mole %) was added to each bowl. DI (De Ionized) water was added to provide a wet medium. Mixing was carried out for 30 mins. Then the samples were dried in an oven. The dried samples were then placed in a alumina crucible and calcined at 600 °C for 4 hours. Calcination was done to convert copper (II) nitrate to copper (II) oxide. If the powders are not calcined, then they will form copper (II) oxide while firing, forming excess pores that cannot be easily removed easily.

15 g of these calcined powders was taken in an agate mortar. Few drops of Poly Vinyl Alcohol (PVA)(5%) was added as binder to it. Two batches of different weights of powder were taken; 0.7 grams of powder for preparing dilatometry bars and 1 gram of powder for preparation of pellets. Powders were pressed in a rectangular die (of length 15 mm length) to form dilatometry

bars and in a circular die (of dia 12.5 mm) to form pellets. Pressing was done at 4.5 tons with a dwell time of 90 seconds.

Firing was done at different temperatures; 1100 °C, 1200 °C, 1400 °C, 1550 °C and 1650 °C. Soaking time was 4 hours for each firing temperature. At 1650 °C isothermal heating of the samples was done at different soaking times; 2 hrs, 4 hrs, 6 hrs, 8 hrs, 10 hrs and 12 hrs. This whole process has been characterized in Fig 1.

3.7 CHARACTERIZATION :

Dry , soaked and suspended weights were calculated for the samples using Archimedes principle to calculate the bulk density of the sintered pellets. Prior to the calculation the pellets were placed in a vacuum for 1 hour. It was calculated using this formula:

$$\text{Bulk Density} = \frac{\text{dry weight}}{(\text{soaked weight} - \text{suspended weight})} * \text{Density of the liquid.}$$

Apparent porosity is a calculation of the amount of open pores in a body. It can also be calculated from dry , soaked and suspended weight based on Archimedes principle.

$$\text{Apparent porosity (AP)} = \frac{(\text{soaked weight} - \text{dry weight})}{(\text{soaked weight} - \text{suspended weight})} * 100\%.$$

It is expressed as a percentage.

Rectangular bars of approximately 15.21 mm are pressed and then subjected to firing at different temperatures at constant heating rate (CHR) of 5 °C/min , 10 °C/min and 15 °C/min respectively. This is used to study the shrinkage behaviour with temperature / time (CHR). The bars were first heated to a temperature of 1200°C and later to a temperature of 1450°C. As dilatometer machine can measure continuous change in length over a large range of temperature, its results can be used to calculate activation energy.

SEM samples were subjected to ultrasonication in acetone. SEM analysis was carried out in JEOL-JSM 6480LV at applied generator voltage of 15 KV. For good SEM images the samples were coated with a layer of platinum by sputtering and they were grounded with the help of carbon tapes.

CHAPTER 4

RESULTS AND DISCUSSION

4.1 Densification Analysis:

Pelletized samples were made and fired at different temperatures and bulk densities were measured at different temperatures: 1100 °C, 1200 °C, 1400 °C, 1550 °C, 1650 °C for 4 hours.

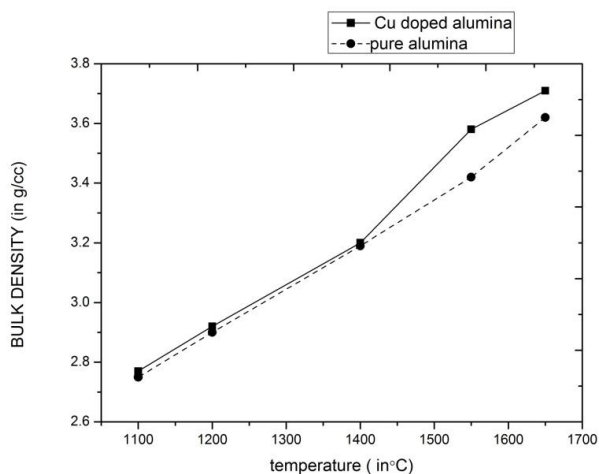


Fig 2. Plot of Bulk Density vs Firing Temperature (soaking time: 4 hrs)

From fig 2. we can observe that no measurable change in density was observed upto 1400 °C. But clear change in densification at 1550 °C and 1650 °C can be observed. Maximum density was obtained for Cu doped Alumina samples at 1650 °C with soaking time 4 hours as 3.71 gm/cc

(93.2% dense) and that for undoped samples was 3.62 g/cc(91 % dense).

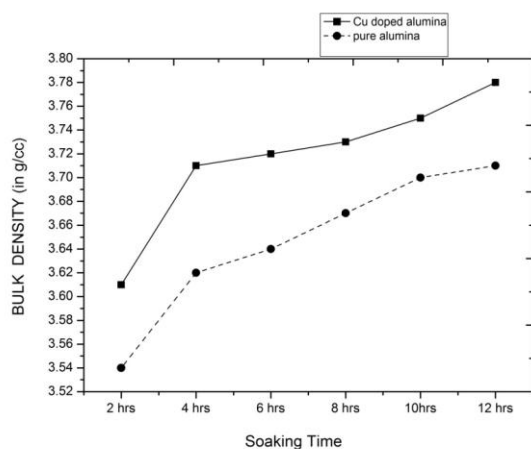


Fig 3. Plot of Bulk Density with soaking time (temperature : 1650 °C)

All the above samples have been fired isothermally at 1600 °C with different soaking times ranging from 2 to 12 hours with an interval of 2 hours. Maximum density were obtained for Cu doped Alumina samples 1650 °C with

soaking time 12 hours as 3.78 gm/cc (95.2%) and that for undoped samples was found to be 3.71(92.3 % dense). Though we observe that the difference in maximum density is only 2 % but this is due to the less quantity of dopant that we have used. Still, the results predict that with addition of copper to alumina densification increases. This has been shown in Fig 3.

Apparent porosities for doped as well as undoped alumina samples fired at 1100 °C, 1200 °C, 1400 °C, 1550 °C, 1650 °C for 4 hours were also calculated.

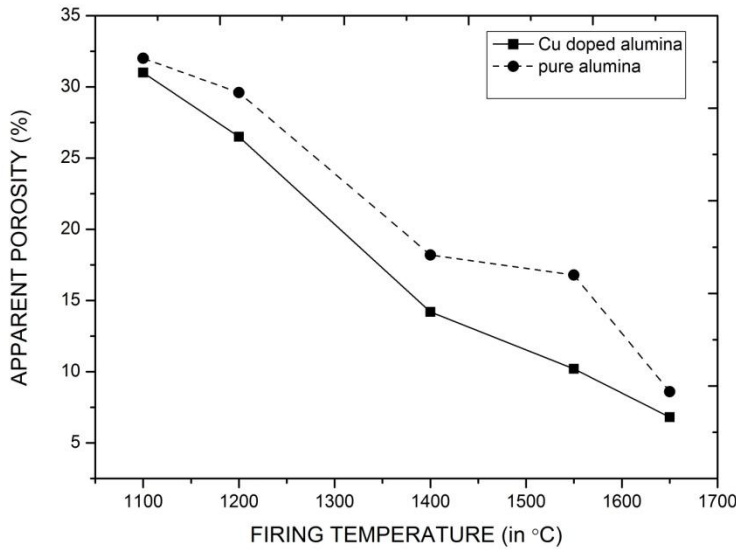


Fig 4. Plot of Apparent Porosity with Firing temperature (soaking time : 4 hrs)

In fig 4. apparent porosity was found to be least for 1650 °C (soaking time= 4 hours), that is 6.8 % for Cu doped alumina samples and that for undoped samples it was 8.6%.

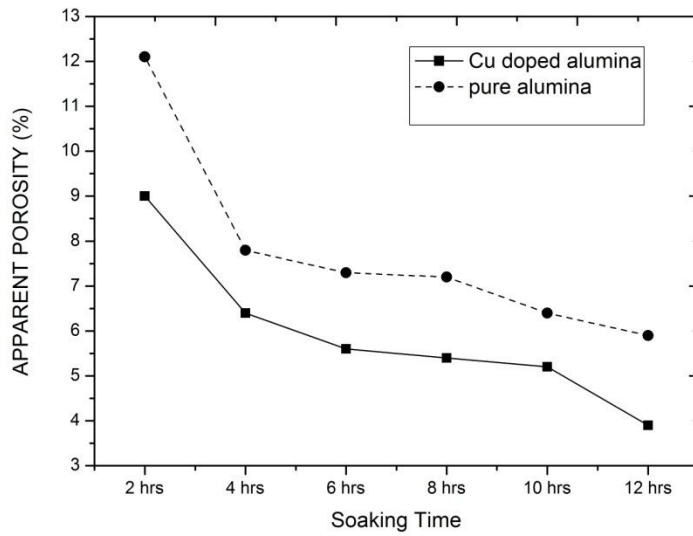


Fig 5. Plot of Apparent Porosity with Soaking time (temperature : 1650°C)

Apparent porosity was also calculated for isothermally sintered samples. From fig 5. apparent porosity was found to be 3.9% for Cu doped alumina samples fired at 1650°C at 12 hrs. and that for undoped samples was found to be 5.9%. These results are consistent with the theory that addition of copper helps in improving densification which we have showed from fig 2 and fig 3.

4.2 Dilatometric Study:

Dilatometry was carried out at a constant heating rate of 5 °C/min upto 1450 °C on doped samples. As it can be seen from fig 6(a) that temperature at which sintering starts = 975 °C. When the samples are heated there is an expansion in length recorded by the machine caused by linear thermal expansion with temperature observed at low temperatures. At around 800 °C decomposition of PVA takes place and is removed as volatile matters. This causes a sudden increase in the expansion of the sample. Then around 975 °C, densification starts. The densification achieved was almost ~ 4 %. Such levels of sintering can be indicative of the initial

stage sintering stage.

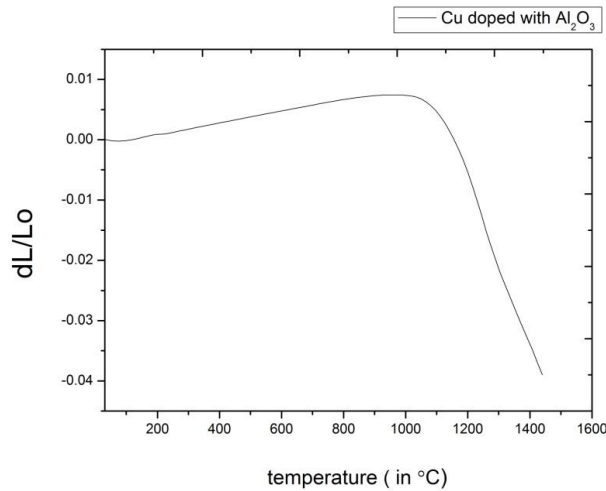


Fig 6(a). Plot of dL/Lo (shrinkage) with temperature (at 5 °C/min)

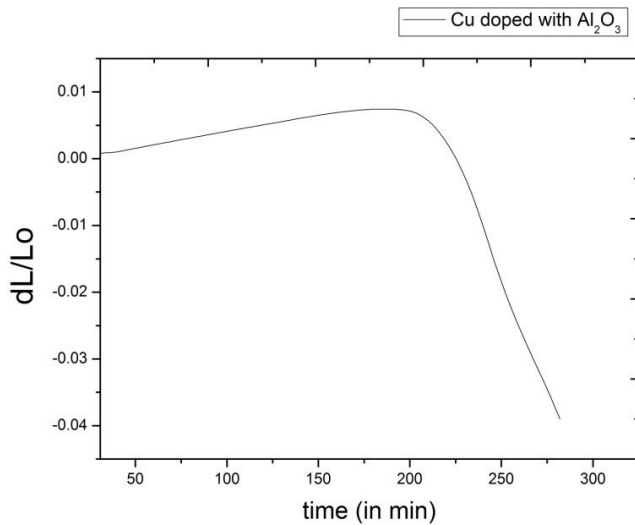


Fig 6(b). Plot of shrinkage (dL/Lo) with time (at 5 °C/min)

Dilatometry was again carried out at a higher constant heating rate of 10 °C/min upto 1450 °C. From fig 7(a) we can observe that temperature at which sintering starts = 1042 °C. Almost 3 % densification was achieved in the samples. The densification here is low as compared to that achieved for 5 °C/min as at higher heating rates the furnace gets heated quickly as compared to the sample. So furnace temperature rises quickly to 1450 °C but the sample temperature is much lower than that, thus less densification is achieved. Other than this, the graph characteristics are same as that achieved for 5 °C/min.

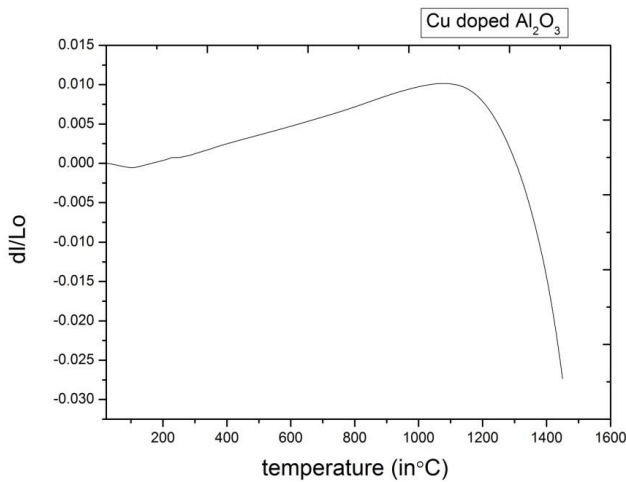


Fig 7(a). Plot of shrinkage with temperature (at 10 °C/min)

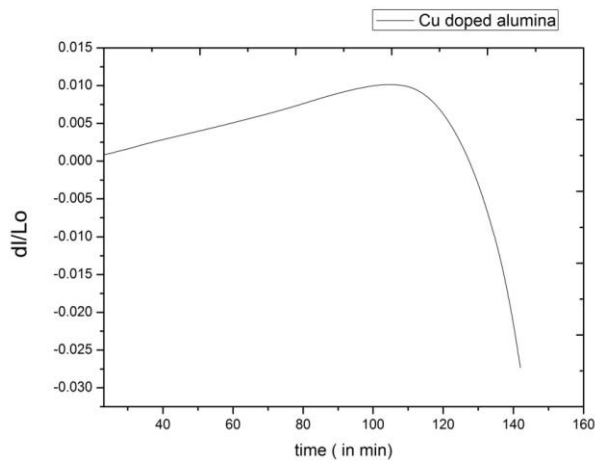


Fig 7(b). Plot of shrinkage (dL/Lo) with time (at 10 °C/ min)

Dilatometry was carried out at an even higher constant heating rate of 15 °C/min upto 1450 °C. From fig 8(a), the observed temperature at which sintering starts = 1081 °C. The starting temperature of sintering has increased even further, the reason being the same as explained for 10 °C/min. Almost 3 % densification was achieved. Such densification values was indicative of initial stage sintering. Apart from a slight change in the readings, the graph characteristic is more

or less the same as the previous two dilatometric graphs.

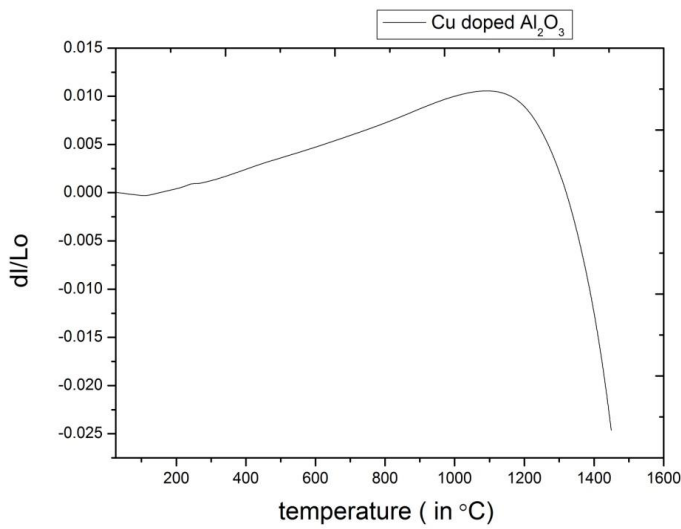


Fig 8(a). Plot of shrinkage (dL/Lo) with temperature (at 15 °C/min)

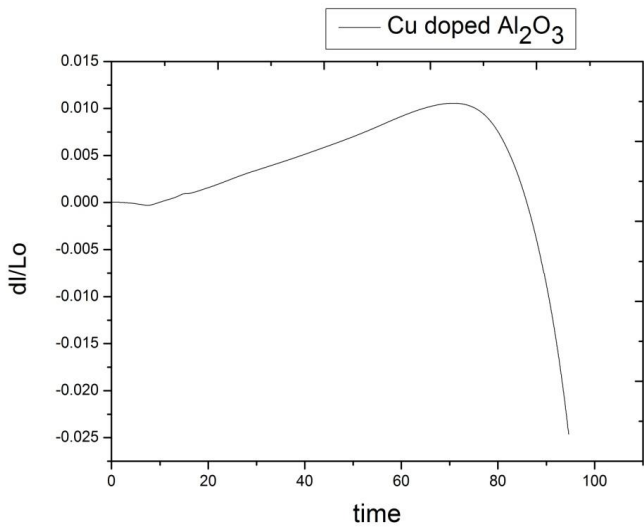


Fig 8(b). Plot of shrinkage (dL/Lo) with time (at 15 °C/ min)

In fig 9(a) dilatometric curves for doped alumina samples are shown for the all the 3 different heating rates together. Here when we compare all the 3 graphs we can see that all 3 graphs have the same characteristics, that is after an initial shrinkage which has the same value for all three heating rates, they all show similar types of curves. An interesting thing of note is that the curves for 10 °C/min and 15 °C/min are more closer than the curves of 10 °C/min and 5 °C/min. It is indicative of faster densification at 5 °C/min than at higher heating rates.

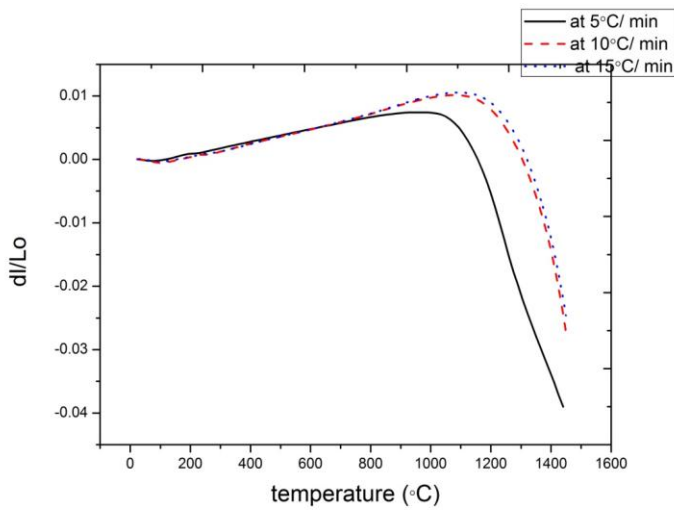


Fig 9(a). Plot of shrinkage (dL/Lo) with temperature for different heating rates.

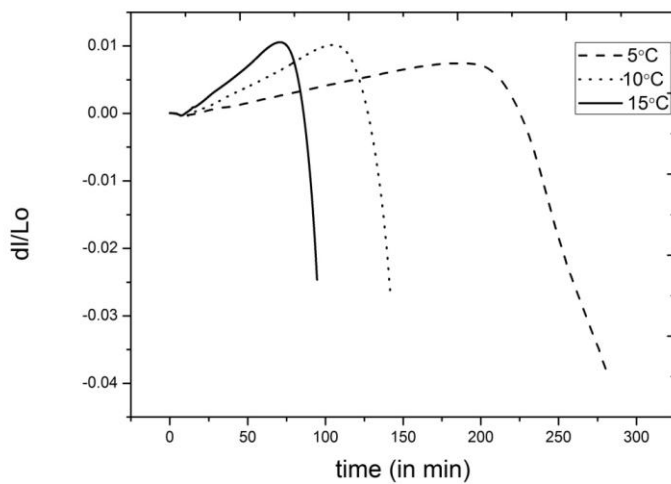


Fig 9(b). Plot of shrinkage (dL/Lo) with time for different heating rates.

4.3 Calculation Of Activation Energy:

The generalized form of neck growth can be expressed from the two-sphere densification/sintering model [22,23].

$$\left(\frac{X}{Rp}\right)^n = \frac{Bt}{Rp^m} \longrightarrow \text{eqn 1}$$

where, X is the neck radius, Rp is the particle radius, t is the time, m and n are constants and the value of m and n depended on the kinetic mechanism of the initial stage of sintering, $B = B_0 T^a$, where B_0 corresponds to the combined material and numerical constants and is related to the temperature (T) through the Arrhenius law. The exponent n (kinetic constant) of Eqn. (1) identifies the sintering mechanism. The value of n for different mechanism and the corresponding values of the temperature exponent 'a' have been given in Table 2.

The neck growth and the shrinkage for the densification can be correlated by Eqn. (2), where, L_0 is the initial dimension of the green compact and ΔL is the shrinkage at time t.

$$\frac{\Delta L}{L_0} = \left(\frac{X}{2Rp}\right)^2 \longrightarrow \text{eqn (2)}$$

Equation (1) and (2) can be combined to yield Eqn. (3)

$$\frac{\Delta L}{L_0} = \left(\frac{B_0 T^a t}{2^n R_p^m}\right)^{2/n} \longrightarrow \text{eqn (3)}$$

and this describes the densification behavior for isothermal conditions.

Table No 1. Dependence of frequency factor with temperature corresponding to the kinetics models used in literature [23]

Kinetic Model	a	n
Viscous flow	0	2
Plastic flow	-1	2
Volume diffusion	-1	5
Grain boundary diffusion	-1	6
Evaporation condensation	-3/2	3
Surface diffusion	-1	7

The time derivative of Eqn. (3) is

$$\frac{d(\Delta L/L_o)}{dt} = \frac{d}{dt} \left(\frac{B_o T^a t}{2^n R_p^m} \right)^{2/n} \longrightarrow \text{eqn (4)}$$

$$= k \left(\frac{\Delta L}{L_o} \right)^{1-n/2}$$

where, $k = B_o T^a / 2^{n-1} n R_p^m$. B_o can be expressed by the Arrhenius type relationship

$$k = A e^{-Q/RT} \longrightarrow \text{eqn (5)}$$

where, Q is the activation energy and $A = A_o T^a$. The pre-exponential factor (A) of the Arrhenius equation is dependent on the exponent 'a' describing the dependence with the absolute temperature T . Substitution of Eqn. (5) into eqn. (6) results in the following equation

$$\frac{d(\frac{\Delta L}{L_0})}{dt} = A_0 T^a e^{-Q/RT} \left(\frac{\Delta L}{L_0}\right)^{1-n/2} \longrightarrow \text{eqn (6)}$$

Equation (6) describes the time rate of shrinkage $\Delta L/L_0$ at a certain temperature and gives the generalized expression applicable for both isothermal and non-isothermal densification condition [24-26]. Thus, any set of data $d(\Delta L/L_0)/dt$ - T - $\Delta L/L_0$ should fit Eqn. (6) independent of the experimental conditions (i.e., isothermal, non-isothermal conditions).

The dilatometric curve obtained from a linear-heating rate ($\beta = dT/dt$), i.e., non-isothermal condition can be described by the Eqn. (8) (which is obtained by integrating (7) followed by rearrangement).

$$T^2 \frac{d(\frac{\Delta L}{L_0})}{dt} = \frac{2\beta Q}{nR} \left(\frac{\Delta L}{L_0}\right) \longrightarrow \text{eqn (7)}$$

Freeman and Carroll [27] proposed that the sintering kinetics could be determined from a single CRH curve by using the given formula :

$$\frac{d \ln \left(\frac{d(\frac{\Delta L}{L_0})}{dt} \right)}{d \ln \left(\frac{\Delta L}{L_0} \right)} - a \left(\frac{d \ln(T)}{d \ln \left(\frac{\Delta L}{L_0} \right)} \right) = \left(\frac{Q [d(\frac{1}{T})]}{R [d \ln \left(\frac{\Delta L}{L_0} \right)]} \right) + 1 - \frac{n}{2} \longrightarrow \text{eqn (8)}$$

Where Q = Activation Energy

R = universal gas constant

dL/L_0 = shrinkage

n = Avrami coefficient

a = constant

T = Absolute Temperature

For a fixed value of 'a', the plot of LHS of Eqn. (8) against $d(1/T)/d \ln(\Delta L/L_0)$ yields a straight line whose slope is Q/R and $(1 - n/2)$ is the intercept. The straight line thus obtained gives Q/R as slope and $(1 - n/2)$ as the intercept. Thus, Q and n can be simultaneously determined from this model. (Eqn. (8)) using a single dilatometric curve. However, the parameter 'a' is to be assumed from the Table-2 for fitting into these equations.

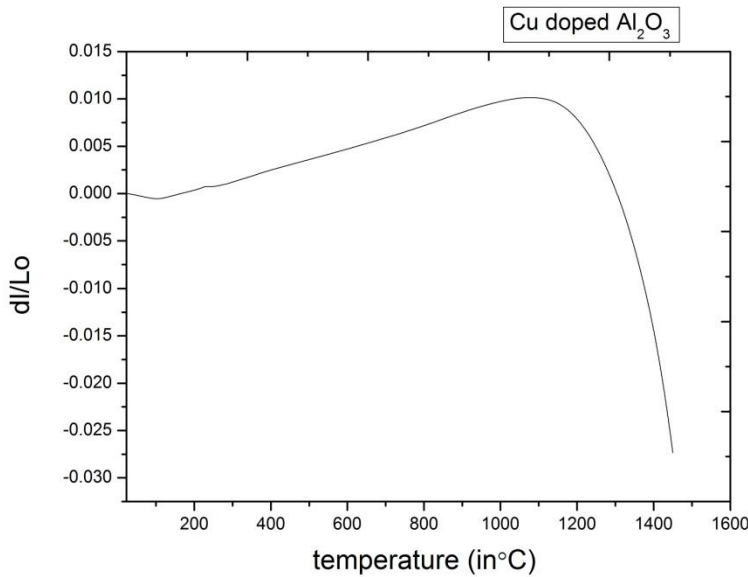


Fig 10. Plot of a dilatometric curve for constant heating rate.

For calculating activation energy, we have to do some changes in the dilatometric plot. We need to plot it again but from where densification starts. We have to find the dL (marked as x) at that point and calculate $dL/(L_0 + x)$ which will give a new plot of shrinkage (dL/L_{new}).

Then we calculate the data according to this new shrinkage value. Here we assume 'a' as -1.

Table No. 2: Values of X And Y Axes for Activation Energy Plot:

$\frac{[d(\frac{1}{T})]}{[d\ln(\frac{dl}{Lo})]}$	$\frac{d\ln(\frac{d(\frac{dl}{Lo})}{dt})}{d\ln(\frac{dl}{Lo})} - a\left(\frac{d\ln(T)}{d\ln(\frac{dl}{Lo})}\right)$
-2.78569E-7	0.00552
-2.31117E-6	0.04737
-4.39535E-6	0.15444
-8.0134E-6	0.23547
-1.13491E-5	0.39024
-1.30175E-5	0.02112
-1.45129E-5	0.28209

We first plot the graph as a scatter plot:

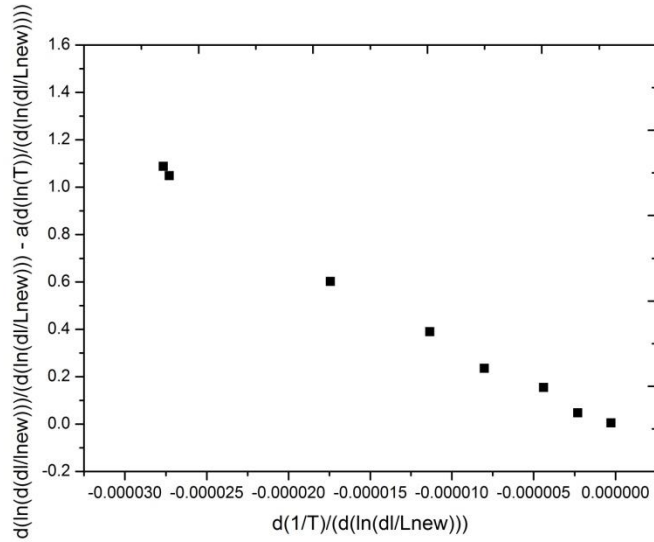


Fig 11. Plot of scatter points for activation energy calculation.

Then we linearly fit the points as such .regression coefficient is near 1.

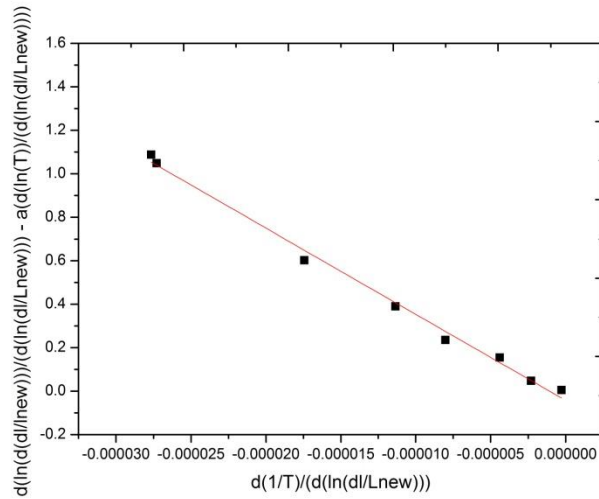


Fig 12. Plot of activation energy graph.

Now the slope is calculated which gives us the activation energy.

$$\text{Slope} = (Q/R) = -39627.865$$

$$\text{Therefore, } Q = 39627.865 * R = 39627.865 * 8.314 = 329.45 \text{ kJ/mole} \sim 330 \text{ kJ/mol}$$

Regression coefficient was found to be 0.99.

We have found that activation energy for pure alumina from literature [24] was found around $440 \pm 40 \text{ kJ/mole}$.

4.4 Scanning Electron Microscopy:

Isothermally sintered samples at 1650 °C were analysed with SEM to study its microstructure. Unlike dilatometry samples which were heated in an inert atmosphere, samples fired in a furnace are heated in an oxidising atmosphere. Dilatometric samples are supposed to contain metallic copper, though we have no proof. In an oxidising atmosphere, Cu forms copper oxide which is a low melting phase. But as we have added only a minuscule amount of CuO, we do not observe significant changes in densification. The changes in creep properties due to transitional metal oxide doping has been observed by a few research groups (eg. University of Utah, R.S. Gordon). The changes in densification, may be due to formation of liquid or liquid like phases, although the phase present may be of small dimensions. But we can observe from these SEM samples, how densification of doped samped samples is more with less porosity than undoped samples.

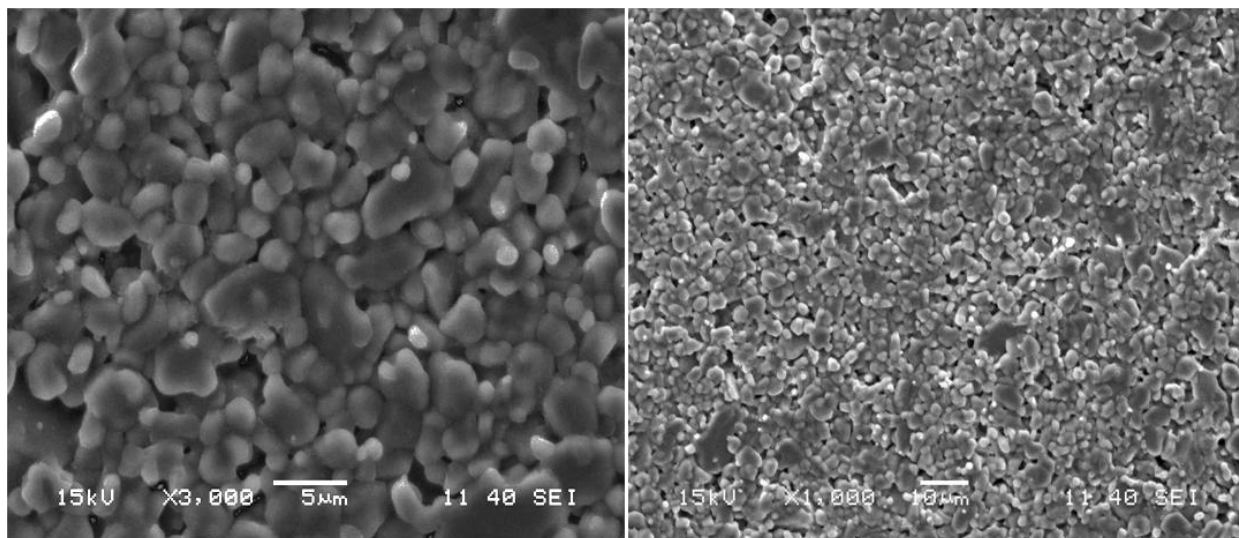


Fig 13. SEM image of Cu doped Alumina fired at 1650 °C with 8 hrs soaking time.

Grain size was found to be approximately between 1.5-2.0 μm

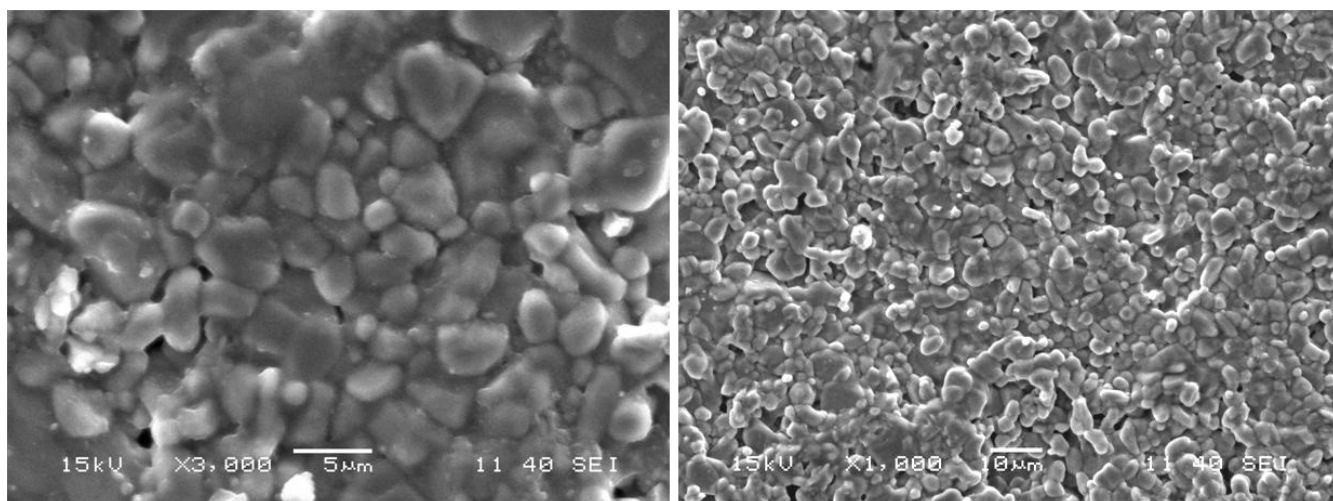


Fig 14. SEM image of Cu doped Alumina fired at 1650 °C with 10 hrs soaking time.

The samples have an average grain size of approximately 2 – 2.5 μm . Here we can see more diffusion than that at 8 hrs soaking time.

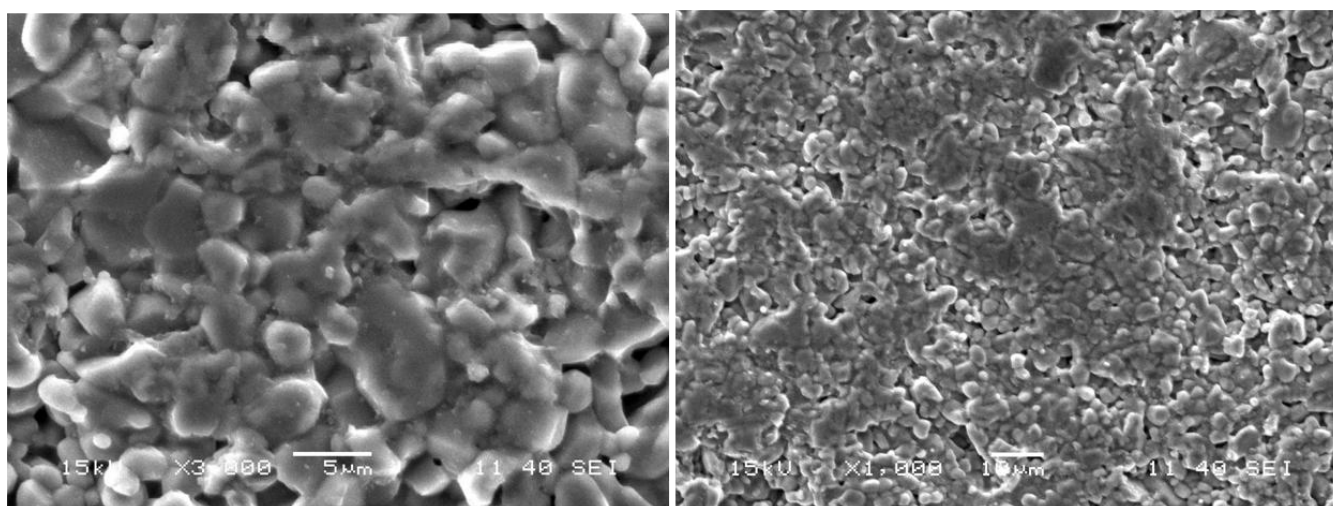


Fig 15. SEM image of Alumina fired at 1650 °C with 10 hrs soaking time.

In comparison with doped samples these samples show more neck growth forming large diffused grains.

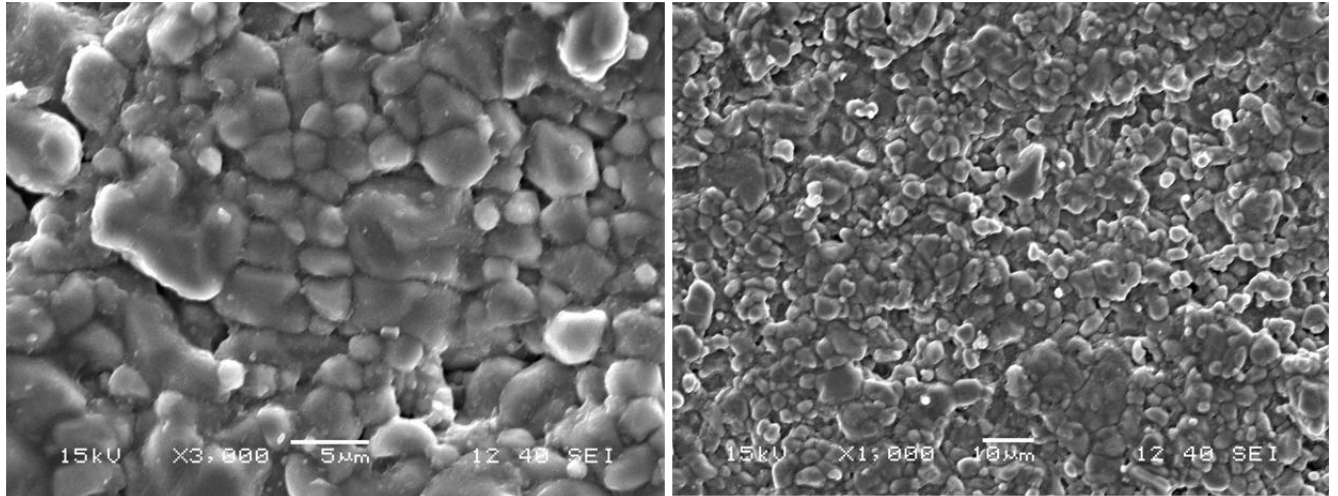


Fig 16. SEM image of Cu doped Alumina fired at 1650 °C with 12 hrs soaking time.

Here we can see more diffusion than at lower soaking time. So we can say that as temperature is increased, the sintering mechanism is more diffusion controlled. The grain size values were found to be near 2.5 –3 μm .

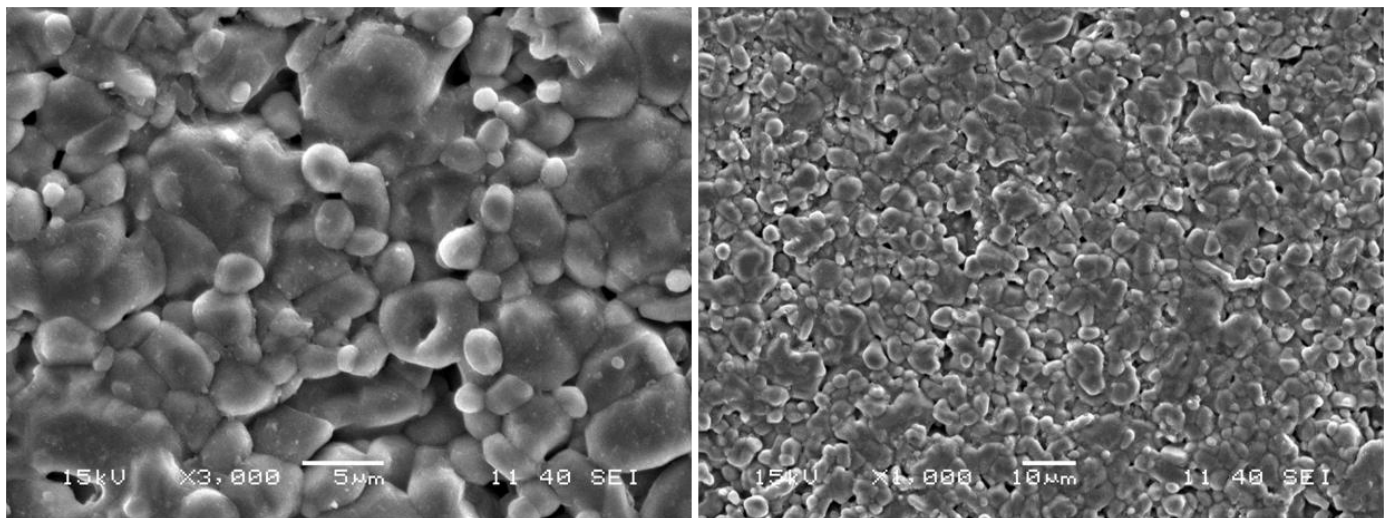


Fig 17. SEM image of Alumina fired at 1650 °C with 12 hrs soaking time

Here most grains have diffused with one another forming very large sized grains.

CHAPTER 5

SUMMARY

- Better densification results were obtained for Cu doped alumina samples than undoped samples. Thus bulk density, apparent porosity and shrinkage studies showed that CuO is effective as a dopant. No appreciable change was observed for sintering in air atmosphere till 1400 °C but after that we can see a clear change in densification values for both doped and undoped samples. A maximum densification of 95 % was obtained for doped samples isothermally fired at 1650 °C for 12 hrs.
- From dilatometric study, we observed that the initial stage of sintering was accelerated for doped samples.
- Activation energy calculated from Arrhenius plots showed that for initial stage of sintering it was around 330 kJ/mol. For undoped samples (pure alumina) activation energy was obtained from literature [28] as 440 k/mol.
- Thus we can theorise that transition metal doping is useful.

REFERENCES

- [1] Heuer, A. M., The role of MgO in the sintering of alumina, *J. Am. Ceram. Soc.*, 62(5-6) (1979), 317-19.
- [2] Rossi, G. And Burke, J. E., Influence of additives on the microstructure of sintered Al_2O_3 , *J. Am. Ceram. Soc.*, 56(12), (1973), 654-9.
- [3] Coble, R. L., Sintering alumina: effect of atmospheres, *J. Am. Ceram. Soc.*, 45(3) (1962), 123-7.
- [4] Brook, R. J., Ceramic fabrication processes, *In Treatise on Materials Science and Technology*, Vol. 9, F. F. Y. Wang (Ed.), Academic Press, New York, 1976, 33144.
- [5] A Botinelli, J Guille, J C Bernier, Densification of alumina at 1400 °C, *Ceramics International* 14 (1988) 31-34
- [6] Hilkat Erkalfa, Ziilal Misirli & Tarik Baykara, Densification of Alumina at 1250°C with MnO_2 and TiO_2 Additives, *Ceramics International* 21 (1995) 345-348
- [7] H. Erkalfa, Z. Misirli, T. Baykara, Effect of additives on the densification and microstructural development of low-grade alumina powders, *Journal of Materials Processing Technology* 62 (1996) 108- 115
- [8] R.J. Coble, *J. Appl. Phys.*, 32 (1961) 793-799.
- [9] M.P. Harmer and R.J. Brook, *J. Mater. Sci.*, 15 (1980) 3017-3024.
- [10] R.J. Brook, *Proc. Br. Ceram. Soc.*, 32 (1982) 7-24.
- [11] S.J. Bennison and M.P. Harmer, *J. Am. Ceram. Soc.*, 68 (1985) C22- 24
- [12] S.J. Bennison and M.P. Harmer, in C.A. Handwerker and W.A. Kaysser (eds.), Sintering of Advanced Ceramics, *J. Am. Ceram. Soc.*, Westerville, OH, 1990, pp. 13-49.
- [13] J.G.J. Pellen, *Mater. Sci. Res.*, 10 (1975) 44C-453
- [14] WC. Johnson and R.L. Coble, *J. Am. Ceram. Soc.*, 61 (1979) 110- 114.

- [15] L. Radonjić, V. Srdić, Effect of magnesia on the densification behavior and grain growth of nucleated gel alumina, *Materials Chemistry and Physics* 47 (1997) 78-84
- [16] Yung-Fu Hsu, Sea-Fue Wang, Yuh-Ruey Wang, Shih-Chueh Chen, Effect of niobium doping on the densification and grain growth in alumina, *Ceramics International* 34 (2008) 1183–1187
- [17] Atsushi Odaka, Tomohiro Yamaguchi, Takayuki Fujita, Seiichi Taruta, Kunio Kitajima, Densification of rare-earth (Lu, Gd, Nd)-doped alumina nanopowders obtained by a sol–gel route under seeding, *Powder Technology* 193 (2009) 26–31
- [18] Atsushi Odaka, Tomohiro Yamaguchi, Takayuki Fujita, Seiichi Taruta, Kunio Kitajima, Densification of Ca-doped alumina nanopowders prepared by a new sol–gel route with seeding, *Journal of the European Ceramic Society* 28 (2008) 2479–2485
- [19] R. Voytovych, I. MacLaren, M.A. Gulgun, R.M. Cannon, M. Ruhle, The effect of yttrium on densification and grain growth in α -alumina, *Acta Materialia* 50 (2002) 3453–3463
- [20] Jewell J. Rasmussen, Gerald B. Stringfellow, Ivan B. Cutler, Sherman D. Brown, Effect of Impurities on the Strength of Polycrystalline Magnesia and Alumina, *J. Am. Ceram. Soc.*, Vol 48, issue 3, (146-150), March 1965.
- [21] Ivan B. Cutler, Cyril Bradshaw, Carl J. Christensen, Edmond P. Hyatt, Sintering of Alumina at Temperatures of 1400°C. and Below, *J. Am. Ceram. Soc.*, Vol 40, issue 4, (134-139), April 1957.
- [22] M. Rahaman, “*Ceramic Processing and Sintering*”. Marcel Dekker, New York, 1995.
- [23] R. German, “*Powder Metallurgy Science*” Metal Powder Industries Federation, Princeton, NJ, 1984.
- [24] M. Brown, D. Dolimore, and A. Galwey, “*Reactions in the Solid State in*

- Comprehensive Chemical Kinetics". *Elsevier, Amsterdam, Netherlands, 1980.*
- [25] A. Galwey and M. Brown, "Thermal Decomposition of Ionic Solids". *Elsevier, Amsterdam, Netherlands, 1999.*
- [26] F. Gotor, J. Criado, J. Malek, and N. Koga, "Kinetic Analysis of Solid-State Reactions: The Universality of Master Plots for Analyzing Isothermal and Nonisothermal Experiments", *J. Phys. Chem., 104, 777–782 (2000).*
- [27] E.S. Freeman and B. Carrol, "Application of Thermo analytical Techniques to Reaction Kinetics: Thermogravimetric Evaluation of Decomposition of Calcium Oxalate Monohydrate," *J. Phys. Chem., 62, 397-394 (1958).*
- [28] Jengdaw Wang, Rishi Raj, Activation Energy For The Sintering Of The Two- Phase Alumina/ Zirconia Ceramics, *J. Am. Ceram. Soc., vol 74, issue 8, 1959-1963, August 1991*